Reprinted from *Guidance and Control 1994*, Volume 86, *Advances in the Astronautical Sciences*, Edited by Robert D. Culp and Ronald D. Rausch, 1994. Published for the American Astronautical Society by Univelt, Incorporated, P.O. Box 28130, San Diego, California 92198, U.S.A.

AAS 94-002

ROTATING UNBALANCED-MASS DEVICES FOR SCANNING: RESULTS FROM THE PROOF-OF-CONCEPT TEST

Dean C. Alhorn* **and Michael E. Polites†**

Rotating unbalanced-mass (RUM) devices are a new way to scan space-based, balloon-borne, and ground-based gimbaled payloads, like x-ray and gamma-ray telescopes. They can also be used to scan free-flying spacecraft. Circular scans, linear scans, and raster scans can be generated. A pair of RUM devices generates the basic scan motion and an auxiliary control system using torque motors, control moment gyros, or reaction wheels keeps the scan centered on the target and produces some complementary motion for raster scanning. Previous analyses and simulation results show that this approach offers significant power savings compared to scanning only with the auxiliary control system, especially with large payloads and high scan frequencies. However, these claims have never been proven until now. This paper describes a laboratory experiment which tests the concept of scanning a gimbaled payload with RUM devices. The test results are compared with those from a computer simulation model of the experiment and the differences are discussed.

INTRODUCTION

Space-based and balloon-borne gimbaled scientific instruments often require scanning to meet their scientific objectives. The same is true of some free-flying spacecraft. For examples, see references 1 to 3. Sometimes, the only possible way to achieve a meaningful scan is to scan the entire instrument or spacecraft. This is true for x-ray and gamma-ray telescopes. The scan patterns required are often linear scans, raster scans, or circular scans. A linear scan is characterized by the instrument or payload line-of-sight repeatedly moving back-and-forth in a line centered on the target. A raster scan is like a linear scan except with some slow complementary motion in a direction perpendicular to the scanning motion. The complementary motion could be a ramp, a saw-toothed waveform, or stepping motion. Circular scans are characterized by the payload line-of-sight repeatedly tracing out a circle centered on a target.

* Aerospace Engineer, Control Electronics Branch, Astrionics Lab, NASA Marshall Space Flight Center, Alabama 35812.

† Research Engineer, Precision Pointing Systems Branch, Structures and Dynamics Lab, NASA Marshall Space Flight Center, Alabama 35812.

Gimbaled payloads mounted to space platforms, like the space shuttle or a space station, can be scanned using gimbal-mounted torque motors. However, this approach requires a great deal of power when the payload is large and the scan frequency is high, because the torque motors must continuously accelerate and decelerate the payload very rapidly. Also, this generates large cyclic reaction torques on the mounting base that can excite local structural resonances, causing scanning or stability problems. To help the stability problem, the mounting base would need to be stiffened, which could add considerable mass to the base. In addition, scanning at high frequencies with some precision can require high gimbal servo bandwidths, which may also be difficult to achieve. A large payload inertia and mass, interacting with any structural flexibility in the gimbals or the torque motors, can produce low-frequency structural resonances which severely limit the servo bandwidth that is attainable with a stable control system. Scanning large payloads at high frequencies means large gimbal torque motors, which have more cogging, ripple, and friction than small ones. With a digital implementation for the gimbal servos, the torque commands to large torque motors have more quantization than those to small torque motors. All of these problems can degrade scanning accuracy. Using control moment gyroscopes (CMG's) or reaction wheels, in place of gimbal torque motors, does not require torquing against the mounting base, but does not eliminate the other problems.

The problems with scanning balloon-borne gimbaled payloads using torque motors, CMG's, or reaction wheels are worse than those just described. Now the gimbaled payload is mounted to a gondola, which has much less mass than the space shuttle or a space station. In fact, it may have less mass than the payload being scanned. What's worse, the gondola attaches to a set of shroud lines, which in turn attaches to a balloon. Therefore, the plant dynamics are extremely complex, which exacerbates the scanning problems.

Obviously, free-flying spacecraft cannot be scanned with gimbal torque motors; but, they can be scanned with CMG's or reaction wheels. The plant dynamics of a free-flying spacecraft are more benign than those of a balloon-borne gimbaled payload, but the other problems with scanning a large payload at high frequencies are just as bad.

References 4 through 7 describe a new approach to scanning space-based and balloon-borne gimbaled payloads, free-flying spacecraft, as well as ground-based gimbaled payloads. It uses a pair of rotating unbalanced-mass (RUM) devices, mounted on the payload or spacecraft, to generate the basic scan motion and an auxiliary control system (ACS) which: (1) keeps the scan centered on the target and (2) produces a complementary motion for raster scanning. The ACS can use gimbal torque motors, CMG's, or reaction wheels, depending on the application, but is not required to have a high bandwidth. Rather, it only has to generate low-frequency, low-amplitude torques to meet its objectives. Thus, large cyclic reaction torques against a mounting base or gondola are avoided when RUM's are used for scanning. The analysis and computer simulation results in references 4 and 5 show that gimbaled payloads and free-flying spacecraft can scan more accurately and with much less power and mass when RUM's are used. However, these claims have never been proven by actual hardware testing, until now.

This paper describes an actual laboratory experiment that tests the concept of scanning a gimbaled payload with RUM devices. Test results from the experiment are presented which prove the concept. The outline of the paper is: (1) summarize the basic theory of scanning with RUM's, (2) describe the laboratory experiment and the procedures for testing the RUM's, (3) present test results for linear and circular scanning with and without RUM's, and (4) offer conclusions and final comments.

THE BASIC THEORY OF SCANNING WITH RUM DEVICES

The basic concept of a RUM device can be explained with the help of Figs. 1 to 3, which show a gimbaled I-beam as an emulated payload to be scanned. A pair of RUM's is mounted on top of the I-beam for linear scanning in cross-elevation. Another pair is mounted on the lower side for circular scanning.

A RUM device is simply a mass, m, on a lever arm, r, rotating at a constant angular velocity,

$$\omega = \frac{2\pi}{T_P} \ , \tag{1}$$

where T_P is the period of rotation of the mass . This generates a centrifugal force, $m\omega^2 r$, on the payload. Mounting the RUM device at a distance, d, from payload center-of-mass generates a cyclic torque, about the center-of-mass, with an amplitude equal to $m\omega^2 rd$.

When the top RUM's in Figs. 1 and 2 are maintained 180 deg out-of-phase as they rotate about the cross-elevation axis (P3), the net torque is cyclic in the cross-elevation axis and has a magnitude of $2m\omega^2 rd$. When the RUM positions are defined by the angle Θ_R in Fig. 3-a and

$$\Theta_R = \omega t = \frac{2\pi}{T_P} t \ , \tag{2}$$

then the net torque in cross-elevation becomes

$$T_X = 2m\omega^2 rd\cos(\Theta_R) = 2m\omega^2 rd\cos\left[\frac{2\pi}{T_P} t\right] \ . \tag{3}$$

Using the definitions for the payload cross-elevation angle Θ_X and elevation angle Θ_E shown in Fig. 4, the payload equation-of-motion in cross-elevation can be approximated by

$$\ddot{\Theta}_X = \frac{T_X}{I} \ , \tag{4}$$

where I is the payload moment-of-inertia in the cross-elevation axis. Equation (4) neglects any friction in the system and assumes perfect cancellation of the reaction torques on the payload caused by any gravity torques on the RUM masses. Substituting eq. (3) into eq. (4) and integrating twice gives the steady-state scan motion:

$$\Theta_X = -\frac{2mrd}{I}\cos\left[\frac{2\pi}{T_P}t\right] = -\rho\cos\left[\frac{2\pi}{T_P}t\right] . \tag{5}$$

As expected, this represents linear scan motion in the cross-elevation axis with an amplitude

$$\rho = \frac{2mrd}{I} \tag{6}$$

and a period T_P, the same as the period of rotation of the RUM's. Hence, changing the lever arm of the RUM devices is a convenient way to change the scan amplitude. Similarly, a simple way to change the scan period is to change the RUM period of rotation, since both are equal to T_P.

When the lower RUM's in Figs. 1 to 3 are maintained 180 deg out-of-phase as they rotate about the payload line-of-sight (P1), the net torque is now cyclic in both the cross-elevation and elevation axes and has a magnitude of $2m\omega^2 rd$. When the RUM positions are specified by the angle Θ_R in Fig. 3-b and Θ_R as a function of time is defined by eq. (2), then the net torques in the cross-elevation and elevation axes are, respectively,

$$T_X = +2m\omega^2 rd\cos(\Theta_R) = +2m\omega^2 rd\cos\left[\frac{2\pi}{T_P}t\right] \tag{7}$$

$$T_E = -2m\omega^2 rd\sin(\Theta_R) = -2m\omega^2 rd\sin\left[\frac{2\pi}{T_P}t\right] . \tag{8}$$

Using the definitions for the payload cross-elevation angle Θ_X and elevation angle Θ_E shown in Fig. 4, the payload equations-of-motion in cross-elevation and elevation can now be approximated by

$$\ddot{\Theta}_X = \frac{T_X}{I} \tag{9}$$

$$\ddot{\Theta}_E = \frac{T_E}{I} \tag{10}$$

respectively, when I is the payload moment-of-inertia in both the cross-elevation and the elevation axes. Again, eqs. (9) and (10) neglect any friction in the system and assume exact cancellation of the reaction torques on the payload caused by any gravity torques on

the RUM masses. Substituting eqs. (7) and (8) into eqs. (9) and (10), respectively, and integrating twice gives the steady-state scan motion

$$\Theta_X = -\frac{2mrd}{I}\cos\left[\frac{2\pi}{T_P}t\right] = -\rho\cos\left[\frac{2\pi}{T_P}t\right] \tag{11}$$

$$\Theta_E = +\frac{2mrd}{I}\sin\left[\frac{2\pi}{T_P}t\right] = +\rho\sin\left[\frac{2\pi}{T_P}t\right] \quad . \tag{12}$$

Clearly, this is circular motion of the payload line-of-sight. The scan radius is ρ and specified by eq. (6); the scan period is T_P, the same as the RUM's period of rotation. Like before, changing the lever arm of the RUM devices is a convenient way to change the scan radius and changing the RUM's period of rotation changes the scan period.

With either linear or circular scanning, the RUM's are required to rotate at a constant angular velocity and stay 180 deg out-of-phase with each other. To achieve this, each RUM device requires a servo with a torque motor and an angular position sensor, like an optical encoder. If the scan rates are not too high, the feedback controller for both servos can be implemented digitally in a single microcontroller; otherwise, analog electronics are recommended. Other implementations for the RUM servos are possible. For example, resolvers can be used in place of encoders; and tachometers could be added for rate feedback.

To keep the RUM-generated scan on target and produce the complementary motion for raster scanning, the ACS is needed. The commands to the ACS need to be synchronized with the motion of the RUM's, so that the ACS does not fight the scan motion generated by the RUM's. For the gimbaled I-beam in Fig. 1, the ACS employs the gimbal torque motors.

The choice of the payload sensors depend on the target to be scanned and the application. For example, if the payload scans the sun, a payload-mounted two-axis sun sensor is recommended. A payload mounted two-axis rate gyro can be added for rate feedback. To simply demonstrate the concept of scanning with RUM devices, gimbal encoders or resolvers are sufficient for position information and gimbal-mounted tachometers can be added for rate feedback. If the RUM servos have a microcontroller, it can also be used to solve the control algorithms for the ACS.

THE EXPERIMENT FOR TESTING RUM DEVICES

Reference 8 presents the conceptual design for a laboratory experiment to test RUM devices for linear and raster scanning a gimbaled payload. Reference 9 describes a similar experiment for circular scanning. These two concepts were combined into one experiment that tests RUM's for all three types of scan patterns. A computer graphic of it is shown in Fig. 1; a photograph of the completed experiment is shown in Fig. 2. The top pair of RUM devices was used for linear and raster scanning and the lower pair was used for

circular scanning. Only one pair of RUM devices was operated at a time and the other pair was mechanically locked and powered down.

In Fig. 2, the control electronics for the servos in the experiment are located on the lab bench in the background. The host computer in the photograph was used to program the microcontroller, which performs the control algorithm computations for the RUM and gimbal servos. In addition, the host computer served several other purposes. It was used to initialize the experiment for scanning; it provided a means to change parameters in the system, like the scan period; and, it was used to retrieve data periodically from the microcontroller and store it on disk. Later, this data was analyzed and plotted to show the performance of the various scans.

In Fig. 2, each RUM has a mass m = 5 lb = 0.155 slugs, on a lever arm r = 0.5 ft, located at a distance d = 2.5 ft from the payload center-of-mass. Mounted on the rotational axis of each RUM device is: a direct-drive brushless DC torque motor with a motor constant K_{MR} = 0.57 ft-lb/$\sqrt{W}$; and an incremental optical encoder, with a resolution of 1.8 arc-min, used to determine the RUM angle.

The payload is a 170 lb, 5 ft long steel I-beam with a 6 in x 6 in cross-section and a flange width of 0.5 in. Including the RUM devices and mounting fixtures, the total payload mass is about 250 lbs. When the payload was circular scanned for a short period of time using only the RUM's, the amplitude of the scan was observed to be about ρ = 51 arc-min = 0.0149 rad. Using eq. 6 and the other known parameters, the moments-of-inertia in cross-elevation and elevation were computed to be about I = 26 slug-ft^2.

The gimbals supporting the payload have a freedom of ±15 deg in cross-elevation and ±90 deg in elevation. On each gimbal axis is: a direct-drive DC torque motor with ±11 ft-lb peak torque, a motor constant K_{MG} = 0.61 ft-lb/$\sqrt{W}$, and a 4 percent ripple torque; an incremental encoder, identical to the ones in the RUM's, for measuring gimbal position; and a tachometer, with 0.48 V/rad/sec sensitivity and 1 percent ripple voltage, to measure the gimbal rate.

All RUM and gimbal servos are controlled by an INTEL 80C196KC microcontroller. It samples all sensor outputs, solves the control algorithms, and issues torque motor commands every T = 7.5 millisec. A control system block diagram for the RUM servos is shown in Fig. 5. Effectively, this is a rate servo with a control law that has proportional, integral, and double integral terms. The control law parameters were selected for a 10 Hz servo bandwidth. The computed torque commands are quantized by 12 bit D/A converters, which are scaled for an LSB of 0.0085 ft-lb. These are issued every computation cycle to the power amplifiers that drive the RUM torque motors. Prior to scanning, the two RUM's being utilized are positioned so the RUM angle, defined by either Fig. 3-a or 3-b, is Θ_R = 0 deg. This properly initializes them to be 180 deg out-of-phase. Once scanning begins, the RUM servos automatically maintain this relationship, when the same commanded change in RUM angle, $\Delta\theta_{RC}$, is issued to each servo every computation cycle. The magnitude of this command determines the period-of-rotation T_P for the RUM's. When $\Delta\theta_{RC}$ is expressed in rad, the governing relationship is:

$$\Delta\theta_{RC} = 2\pi\frac{T}{T_P} \ . \tag{13}$$

The control system block diagrams for the cross-elevation and the elevation servos are shown in Figs. 6 and 7, respectively. For each gimbal servo, the microcontroller reads the incremental encoder output every computation cycle (i.e. every T = 7.5 millisec) and sums these to generate an estimate of the gimbal angle. Each tachometer output is filtered by an analog low-pass filter that rolls off at 46 Hz. The filter output is sampled every computation cycle by a 10 bit A/D converter scaled to a range of ±0.35 rad/sec or ±20 deg/sec. This gives an LSB of about 0.04 deg/sec. Gimbal angle and rate commands are computed in the microcontroller every computation cycle. These are synchronized with the RUM motion so the RUM's and the gimbal servos work together synergistically. This is accomplished by summing the commanded changes in the RUM angle, $\Delta\theta_{RC}$, each computation cycle, in order to generate the commanded RUM angle θ_{RC}. This is shown in Fig. 5. Then, θ_{RC} is input into the computations for the gimbal angle and rate commands shown in Figs. 6 and 7. When only the gimbal servos are used for scanning, the operation is the same except that all four RUM's are mechanically locked and powered down.

For circular scanning, the constants θ_{XCM} and θ_{ECM} were determined to be:

$$\theta_{XCM} = \theta_{ECM} = \rho = 51 \text{ arc-min} = 0.0149 \text{ rad.} \tag{14}$$

Here, ρ was determined by observing the natural scan radius when the RUM's were activated for a short period of time without the gimbal servos. An alternative is to compute ρ using eq.(6), provided the system parameters are accurately known. The constants Ω_{XCM} and Ω_{ECM} were determined to be:

$$\Omega_{XCM} = \Omega_{ECM} = \frac{2\pi}{T_P}\rho = 322 \text{ arc-min/sec} = 5.37 \text{ deg/sec} = 0.0937 \text{ rad/sec} \ , \tag{15}$$

when the scan period T_P = 1 sec, which was the baseline for all tests.

For linear scanning, the only difference is

$$\theta_{ECM} = \Omega_{ECM} = 0. \tag{16}$$

In Fig. 7, specifying the bias elevation angle command θ_{ECO} determines the nominal elevation angle for circular or linear scanning. Varying θ_{ECO} as a function of time generates the complementary motion for raster scanning.

The control law for each gimbal servo is a proportional-integral controller with rate feedback. The control gains were chosen for a servo bandwidth of approximately 0.1 Hz. In fact, structural resonances in the system made it impossible to get a higher bandwidth and still have a stable control system. In the forward loop of each servo is a digital

low-pass filter that rolls off at 2 Hz. It prevents exciting these structural resonances as much as possible. The output of the digital filter is the torque command for the gimbal torque motor. Its magnitude is quantized to 8 bits, with each bit corresponding to about 0.05 ft-lb. The quantized torque command is issued by the microcontroller every computation cycle to a PWM generator, which in turn drives the power amplifier for the gimbal torque motor.

PROCEDURES FOR TESTING THE RUM DEVICES

To test the RUM devices for scanning the payload, a number of scans were performed. Linear and circular scans were generated, with and without RUM devices, at nominal elevation angles of 0 and -90 deg. A 0 deg elevation angle is the best orientation for linear scanning with RUM's, because no gravity torque acts on them. Therefore, this is like a simulated zero-g test for linear scanning with RUM's. A -90 deg elevation angle is the worst orientation for linear scanning with RUM's, because the gravity torque acting on them is a maximum. Just the opposite is true for circular scanning with RUM's. As a result, these two elevation angles cover both extremes for both types of scanning with RUM's. Scanning without RUM's should give similar results at any elevation angle, when the payload is properly mass balanced. Raster scanning to test RUM devices has one drawback. The entire system never truly reaches steady state, because the peak gravity torque on the RUM's continually changes with the changing elevation angle. For this reason, linear and circular scans were used to evaluate scanning with and without RUM's. Raster scanning was observed and verified, but no results are included here.

For a given scan, about two minutes was allowed for the system to reach steady state. Then, over the next 15 sec, the gimbal and RUM servo variables were sent every computation cycle (i.e. every 7.5 millisec) from the microcontroller to the host computer and stored on disk. Later, this data was prepared for plotting. The important criteria for judging the results of scanning, with and without RUM's, are the size of the scan, the scan errors, the torques generated by the torque motors used in the scan, and the power dissipated in these torque motors. For each scan, these performance criteria were determined from the variables sent to the host computer.

The size of the scan was determined from the measured cross-elevation and elevation gimbal angles used in the gimbal servos. These values were obtained by summing the gimbal incremental-encoder outputs in the microcontroller. When the nominal elevation angle was -90 deg, then -90 deg was first subtracted from the stored values for the elevation angles before plotting, in order to give better plot resolution. Then, the gimbal angles were plotted versus time, in the case of a linear scan. They were plotted versus each other, in the case of a circular scan.

The scan errors were determined from the gimbal angle errors in the gimbal servos. These were arrived at by differencing the gimbal angle commands with the measured gimbal angles. The elevation errors were not altered before plotting and both errors were plotted versus time for both linear and circular scanning. In addition, the RMS values of these errors, over the 15 sec intervals, were computed and tabulated, in all cases.

The RUM experiment was not designed to directly measure the torque, current, or power of any motor; so, an indirect method was used to estimate the torque and power of each motor during scanning. This method utilized the torque motor commands in both the gimbal and RUM servos. The torque motor command data was multiplied by an appropriate scale factor that relates the commands to the delivered torque for each motor in order to estimate the actual motor torques. For the RUM torque motors, these scale factors were determined by holding the I-beam fixed, using the gimbal servos, and positioning the RUM masses for a maximum gravity torque (2.5 ft-lb), using the RUM servos. Dividing 2.5 ft-lb by the steady state torque commands in the RUM servos gave the scale factor 0.90 for the RUM torque motors. For the gimbal torque motors, these scale factors were determined by holding the I-beam fixed using the gimbal servos and positioning the RUM's so they were 180 deg out-of-phase and contributed no imbalance torque to the I-beam. One RUM was then rotated 180 deg to produce a known change to the imbalance torque on the I-beam (5 ft-lb). Dividing this torque by the observed change in the torque command for the appropriate gimbal servo, gave the scale factor 0.78 for both gimbal motors. The estimated motor torques were plotted versus time in all cases.

Next, the RMS values for the estimated RUM motor torques, $T_{R1(RMS)}$ and $T_{R2(RMS)}$, were computed over each 15 sec interval. The estimated RMS power dissipated in the RUM motors was computed as follows:

$$P_{R(RMS)} = \left[\frac{T_{R1(RMS)}}{K_{MR}}\right]^2 + \left[\frac{T_{R2(RMS)}}{K_{MR}}\right]^2 , \tag{17}$$

where $K_{MR} = 0.57$ ft-lb/$\sqrt{W}$.

A similar, but slightly different procedure was used for the gimbal motors. Here, the mean and the standard deviation of the estimated gimbal motor torques were computed over each 15 sec interval. Denoting the standard deviations by $T_{X(SD)}$ and $T_{E(SD)}$, the estimated RMS power dissipated in the gimbal motors was computed from the relationship:

$$P_{G(RMS)} = \left[\frac{T_{X(SD)}}{K_{MG}}\right]^2 + \left[\frac{T_{E(SD)}}{K_{MG}}\right]^2 , \tag{18}$$

where $K_{MG} = 0.61$ ft-lb/$\sqrt{W}$. This procedure was used, because better mass balancing of the payload could have eliminated the mean gimbal torques. When the mean is zero, the standard deviation is equal to the RMS. The sum of $P_{R(RMS)}$ and $P_{G(RMS)}$ gave the estimated total RMS power dissipated in all motors used in a given scan. Of course, if the scan is performed without RUM devices, then the RUM motor torques are zero and $P_{R(RMS)} = 0$.

TEST RESULTS FOR LINEAR SCANNING

The procedures just described were used to obtain test results from the RUM experiment for linear scanning, with and without RUM's. Reference 10 contains the actual steady state time responses from the RUM experiment for a linear scan with a 1 sec period, at elevation angles of 0 and -90 deg. These results are summarized in table 1. For comparison, these same cases were run in a simplified computer simulation model that was developed from the block diagrams shown in Figs. 5 to 7. The simulation results are also summarized in table 1, by the numbers in parentheses under the corresponding values from the RUM experiment. In the RUM experiment, scanning with RUM's at a 0 deg elevation angle produced a ±51 arc-min scan accurate to 1 arc-min RMS in the scan axis. The total power dissipated in the motors was only 1 watt RMS. The simulation results compared quite well with these.

When this same scan was attempted in the RUM experiment using only gimbal servos, the amplitude of the scan decreased to ±17 arc-min, the scan error increased to 42 arc-min RMS in the scan axis, and the total power dissipated in the torque motors increased to 79 watts RMS. These results compared fairly well with those predicted by simulation. The amplitude of the actual scan is 23 percent smaller than that predicted by simulation. The torque motor power is 61 percent larger, which means the RMS torques are about 27 percent larger, since torque is proportional to the square root of power. Thus, the two results match fairly well and the differences are certainly in the right directions, since the computer simulation model is simplified. For example, the simulation assumes no payload products of inertia or mass imbalance, no RUM manufacturing or mounting errors, and a value for gimbal friction that may be optimistic (0.2 ft-lb per axis).

Using only the gimbal servos, a ±51 arc-min scan could be generated, if the amplitude of the commands to them were increased by a factor of 2.5 and the gimbal torque motors were approximately doubled in size, from 11 ft-lb to perhaps 22 ft-lb. Using this approach, the extrapolated test results and the corresponding simulation results are shown in table 1. The extrapolated test results show that when the gimbal servos generate a ±51 arc-min scan, the scan error is 105 arc-min RMS in the scan axis and the torque motor power is 494 watts RMS.

Therefore, using the RUM's to help generate a ±51 arc-min linear scan at a 0 deg elevation angle reduces the RMS error in the scan axis by a factor of 105 and reduces the total RMS power dissipated in the torque motors by a factor of 494. The size of the gimbal torque motors can also be reduced, by a factor of 5 or more. Their required peak torque can be reduced from about 22 ft-lb to about 4 ft-lb or less. This means less gimbal motor mass, friction and stiction, cogging and ripple, and better resolution in the torque commands. The reduced mass helps to offset the mass of the RUM devices. The other changes have a positive effect on scan accuracy and power dissipation. Furthermore, the lower reaction torques on the mounting base mean that the base can be less rigid and consequently less massive.

This same methodology was repeated at an elevation angle of -90 deg. In the RUM experiment, a ±51 arc-min scan was generated using both the RUM's and gimbal servos.

The scan accuracy was again 1 arc-min RMS in the scan axis and the motor power dissipated was now 29 watts RMS.

Using only the gimbal servos in the RUM experiment, a ±51 arc-min linear scan was commanded; however, a ±18 arc-min linear scan was actually generated. The scan accuracy was 42 arc-min RMS in the scan axis and required a total torque motor power of 79 watts RMS. If the gimbal servo commands are increased by a factor of 2.5 and the gimbal torque motors are doubled in size, a ±51 arc-min linear scan could be generated. Except now, the scan accuracy is 105 arc-min RMS and the total torque motor power dissipated is 494 watts RMS. These results were derived by extrapolation, as before, and are identical to the extrapolated results at 0 deg elevation angle, as expected.

Thus, using the RUM's to help generate a ±51 arc-min linear scan at a -90 deg elevation angle reduces the RMS error in the scan axis by a factor of 105, reduces the total RMS power dissipated in the torque motors by a factor of 17, and allows the size of the gimbal torque motors to be reduced by a factor of 5 or more. The benefits from smaller gimbal motors were previously indicated. Note that these improvements are at a 1 sec scan period.

With lower scan periods, or higher scan frequencies, the improvements are even greater when the RUM's are used for linear scanning. Without the RUM's, each time the scan period is cut in half, the cross-elevation torque motor needs to generate 4 times more torque and dissipate 16 times more power to produce the same sized linear scan. This can be seen by differentiating eq. 5 twice, substituting this result into eq. 4, and solving for T_X to get

$$T_X = \rho I \left[\frac{2\pi}{T_P}\right]^2 \cos\left[\frac{2\pi}{T_P} t\right]. \tag{19}$$

Therefore, when the scan period T_P is divided by 2, the peak cross-elevation torque increases by a factor of 4. From eqs. (18) and (19), it becomes apparent that reducing the scan period by a factor of 2 increases the power dissipated in the cross-elevation torque motor by a factor of 16.

On the other hand, when the RUM's are used for scanning, the peak motor torques, and consequently the power dissipated in the motors, are virtually the same at any scan period. This is because the RUM's rotate at a constant angular velocity to generate the scan motion. Furthermore, the peak gravity torque on the RUM's and the peak friction torques in the RUM devices, gimbal motors and bearings do not change with the scan period. Thus, the power required to scan with the RUM's is essentially independent of the scan period.

It is becoming obvious that scanning large payloads at high frequencies without RUM's can require gimbal motors that are too big and consume too much power to be practical. For example, using gimbal servos only to generate a ±51 arc-min linear scan with a 0.25 sec period requires a cross-elevation motor with around 350 ft-lbs of peak torque. This motor would have to dissipate over 126 kilowatts of RMS power when

scanning in either one-g or zero-g. When RUM's are used for the same linear scan, gimbal motors with 4 ft-lbs peak torque can be used and the total motor power would be around 29 watts RMS or less in one-g and 1 watt RMS in zero-g.

Also, the amount of motor power required for scanning affects the mass of the electrical system producing this power. To get an idea of the relationship between power and mass in space applications, reference 11 describes the electrical power system for an earth-orbiting spacecraft. The power generation/storage system delivers about 1 kilowatt of usable power and has a 2,000 lb mass, which includes the solar arrays, batteries and cables. As the power it must deliver goes up, so does its mass. Thus, there is a practical limit to the power that the electrical system can produce for scanning.

TEST RESULTS FOR CIRCULAR SCANNING

The same procedures and methodology used for testing and evaluating linear scanning, with and without RUM's, were used for circular scanning.

Figure 8 shows the actual steady state results from the RUM experiment for circular scanning with the RUM's and gimbal servos. The nominal elevation angle is 0 deg and the scan period is 1 sec. These results are summarized in table 2. They show that a 55 arc-min radius circular scan was generated with a scan error of 4 arc-min RMS or less in each axis. The total power dissipated in the four torque motors used for scanning was 32 watts RMS.

For comparison, this same case was run with the computer simulation model of the RUM experiment for circular scanning. These results are shown in Fig. 9 and are again summarized in table 2, by the numbers in parentheses just under those from the actual RUM experiment. The two results compare fairly well, since the RMS scan errors were within a factor of 2 of each other. Also, the actual power required by the torque motors was 52 percent more than predicted by simulation, which means the RMS torques are just 23 percent larger. This difference is to be expected, since the computer simulation model is simplified in some respects, as previously indicated. The peak elevation torques are about a factor of 3 larger than the peak cross-elevation torques in Fig. 8. This is attributed to a residual mass unbalance of the payload in the P3 direction, which affects the elevation torque primarily. This torque difference should be eliminated by better payload mass balancing.

This same circular scan was attempted in the actual RUM experiment using only gimbal servos. These results are presented in Fig. 10 and are summarized in table 2. The scan never reaches a steady state condition, because of motion in the elevation axis. The radius of the scan about this motion is approximately 18 arc-min, the scan errors are 42 arc-min RMS or more in each axis, and the power dissipated in the gimbal torque motors is 147 watts RMS. The simulation results for this case are also summarized in table 2 and follow the same pattern previously observed when comparing the simulation results with the actual test results.

Again, if the magnitude of the gimbal servo commands were increased by a factor of 2.5 and the gimbal torque motors were doubled in size, then a circular scan with a

51 arc-min radius could be generated using only the gimbal servos, although its center may still wander. By extrapolation, the predicted results for this case are summarized in table 2. The scan error is now 105 arc-min RMS or more in each axis and the total torque motor power is 919 watts RMS. Therefore, using the RUM's to help generate the circular scan at 0 deg elevation angle reduces the RMS scan error in each axis by a factor of 26 or more and reduces the total torque motor power by a factor of 29. The required peak gimbal torque is reduced from around 22 ft-lb to approximately 4 ft-lb; thus, the size of the gimbal torque motors can be reduced by a factor of 5 or more. The benefits of smaller gimbal motors were previously stated.

This same methodology was repeated at an elevation angle of -90 deg. These results are included in reference 10 and are summarized in table 2. The data shows that a 55 arc-min radius circular scan is generated in the RUM experiment when the RUM's are used. The scan errors are 4 arc-min RMS in each axis and the total motor power is 4 watts RMS. The simulation results for this same case are also summarized in table 2; they compare quite well with the actual test results.

Attempting the same scan with the gimbal servos only generates a 20 arc-min radius circular scan, in the RUM experiment. The scan errors are 42 arc-min RMS or more in each axis and the total motor power is 144 watts RMS. Extrapolating these results, like before, gives a 51 arc-min radius circular scan that has a scan error of 105 arc-min RMS or more in each axis and a total motor power of 900 watts RMS. Again these results are obtained when the gimbal servo commands are increased by a factor of 2.5 and the gimbal torque motors are doubled in size.

Therefore, using the RUM's to help generate the same approximate scan at a -90 deg elevation angle reduces the RMS scan error in each axis by a factor of 26 or more and reduces the total motor power by a factor of 225. The peak torque required of the gimbal motors can be reduced from about 22 ft-lb to about 4 ft-lb. Thus, the size of the gimbal motors can be reduced by a factor of 5 or more, which offers the same benefits previously enumerated. Again, it is emphasized that these are the improvements at a 1 sec scan period.

At smaller scan periods, the improvements are even greater when the RUM's are used for circular scanning. Without the RUM's, each time the scan period is divided by 2, both the cross-elevation and the elevation motors need to generate 4 times more torque and dissipate 16 times more power to produce the same sized circular scan. These changes can be proven by the same argument used for linear scanning. Only now, the argument applies to both the cross-elevation and the elevation axes. Thus, each time the scan period is decreased by a factor of 2, the power dissipated in the gimbal motors increases by a factor of 16, when only the gimbal servos are used for circular scanning. Using the same argument as before, the power required to circular scan with RUM's is virtually independent of the scan period.

Again, it is apparent that scanning large payloads at high frequencies without RUM's can require huge gimbal motors that consume too much power to be practical. For example, using gimbal servos only to generate a 51 arc-min radius circular scan with a 0.25 sec period requires gimbal motors with about 350 ft-lbs of peak torque. These

motors would have to dissipate a total power that exceeds 230 kilowatts of RMS power when scanning in either one-g or zero-g. When RUM's are used to generate the same circular scan, gimbal motors with 4 ft-lbs peak torque can be used and the total motor power would be around 32 watts RMS or less in one-g and 1 watt RMS in zero-g.

CONCLUSIONS AND COMMENTS

The test results prove that rotating unbalanced-mass (RUM) devices can be used to generate accurate linear and circular scans for gimbaled payloads in zero-g and one-g, with very little power. Also, extending the results presented here to free-flying spacecraft is straightforward.

Since the results from the simplified computer simulation model of the RUM experiment agreed fairly well with the results from the actual RUM experiment, the basic theory of scanning with RUM devices is verified. This allows the results presented here to be scaled for larger and smaller payloads scanning at higher and lower frequencies.

When the RUM's are used and the scan period is changed, the total motor power and the size of the gimbal motors are virtually unaffected. However, without the RUM's, each time the scan period is reduced by a factor of 2, the peak torque and power of the gimbal motors used in scanning increase by factors of 4 and 16, respectively.

Furthermore, the gimbal motors are more likely to wear out sooner when they must continuously accelerate and decelerate the payload. The increased power dissipation also generates more internal heat, which adversely affects their performance and shortens their lifetime. When the RUM's are used, the gimbal motors work very little and the RUM's rotate at a constant velocity, so all the motors should last a long time.

This experiment proves that it is now feasible to accurately and reliably scan large payloads at high frequencies with significantly less power and significantly less mass, when RUM's generate the basic scan motion. Furthermore, since scanning with RUM's is not founded on torquing against a base structure, it also means that large payloads can scan at high frequencies in places where this was once impossible. For example, consider balloon-borne payloads or free-flying spacecraft.

As a result of this experiment, RUM's are now a proven technology that have known applications in space and have potential applications in defense, industry, and medicine. For example, RUM's may have potential application in military fire control systems for dithering gun barrels. In industry, they have potential applications in spraying water for fighting forest fires or spraying liquid fertilizers and pesticides in open fields. RUM's require so little power that batteries or solar cells could be used as an energy source in remote locations. Also, RUM's could be used in spray painting with a fragile robot arm, because they generate virtually no reaction torques on the arm. In medicine, they may be used for precisely scanning medical devices with considerably less power.

REFERENCES

1. M.E. Nein and P.D. Nicaise, "Experiment Pointing Subsystems (EPS) Requirements for the Spacelab Missions." NASA TM X-64978, NASA Marshall Space Flight Center, AL, December 1975.

2. "The GRID on a Balloon Definition Study Report." NASA Goddard Space Flight Center, Greenbelt, MD, June 14, 1989.

3. "Space Telescope Moving Target and Scan Pointing Capability Error Budget, ST/SE-24, Section H, Part 4." LMSC/FO61415, Lockheed Missiles and Space Company, Sunnyvale, CA, October 21, 1985.

4. M.E. Polites, "Rotating-Unbalanced-Mass Devices for Scanning Balloon-Borne Experiments, Free-Flying Spacecraft, and Space Shuttle/Space Station Experiments." NASA TP-3030, NASA Marshall Space Flight Center, AL, June 1990.

5. M.E. Polites, "New Method for Scanning Spacecraft and Balloon-Borne/Space-Based Experiments." Journal of Guidance, Control and Dynamics, vol. 14, No.3, May–June 1991, pp. 548–553.

6. M.E. Polites, "Rotating-Unbalanced-Mass Devices and Methods for Scanning Balloon-Borne-Experiments, Free-Flying Spacecraft, and Space Shuttle/Space Station Attached Experiments," U. S. Patent # 5,129,600, National Aeronautics and Space Administration, Washington, D.C., July 14, 1992.

7. M.E. Polites and D.C. Alhorn, "Suspension System for Gimbal Supported Scanning Payloads," U. S. Patent Application # 08/123629, National Aeronautics and Space Administration, Washington, D.C., September 15, 1993.

8. W.D. Lightsey, D.C. Alhorn, and M.E. Polites, "Definition and Design of an Experiment to Test Raster Scanning With Rotating Unbalanced-Mass Devices on Gimballed Payloads." NASA TP-3249, NASA Marshall Space Flight Center, AL, June 1992.

9. M.E. Polites and D.C. Alhorn, "Reconfiguring the RUM Experiment to Test Circular Scanning With Rotating Unbalanced-Mass Devices on Gimballed Payloads." NASA TP-3282, NASA Marshall Space Flight Center, AL, September 1992.

10. D.C. Alhorn and M.E. Polites, "Results of a Laboratory Experiment That Tests Rotating Unbalanced-Mass Devices for Scanning Gimbaled Payloads and Free-Flying Spacecraft." NASA TP, NASA Marshall Space Flight Center, AL, to be published.

11. "SIRTF at Higher Altitudes," internal document prepared by the Program Development Directorate, NASA Marshall Space Flight Center, AL, December 1987.

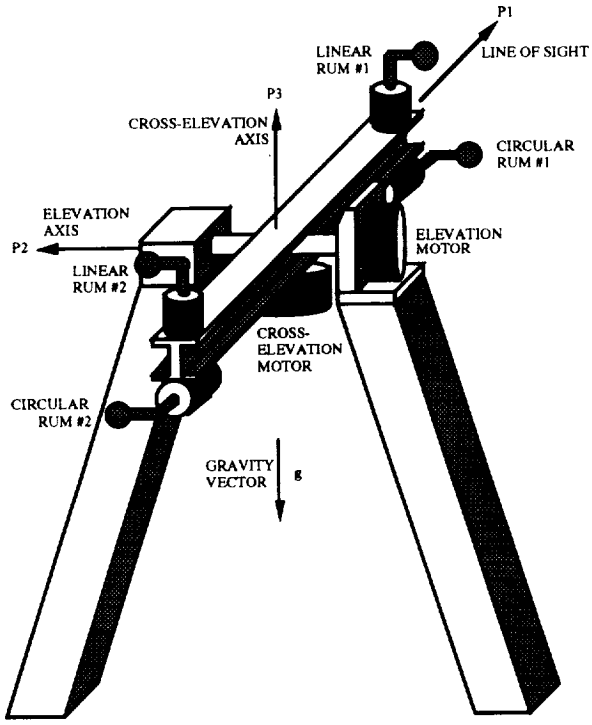

Fig. 1 Concept of an Experiment to Test RUM Devices for Linear, Raster, and Circular Scanning

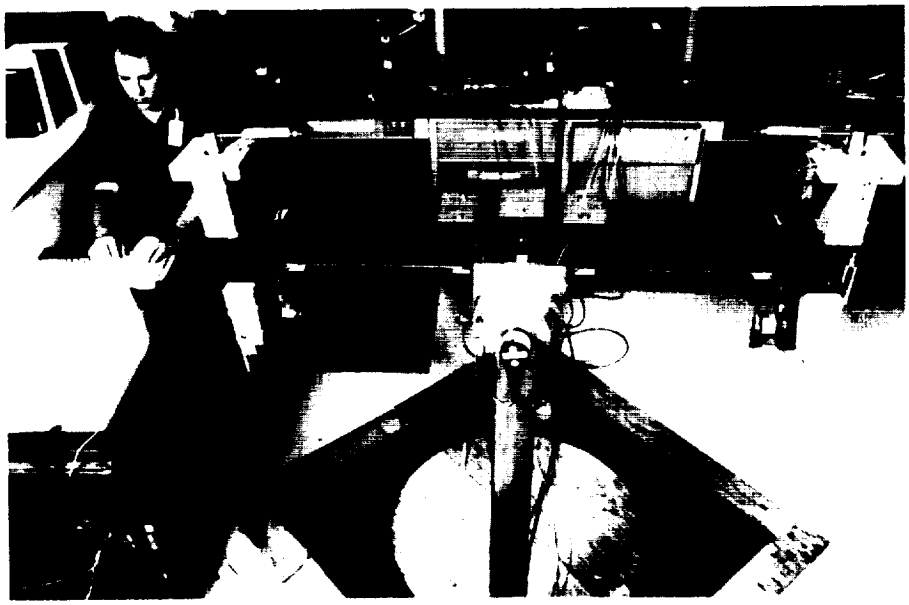

Fig. 2 Photograph of the Completed RUM Experiment

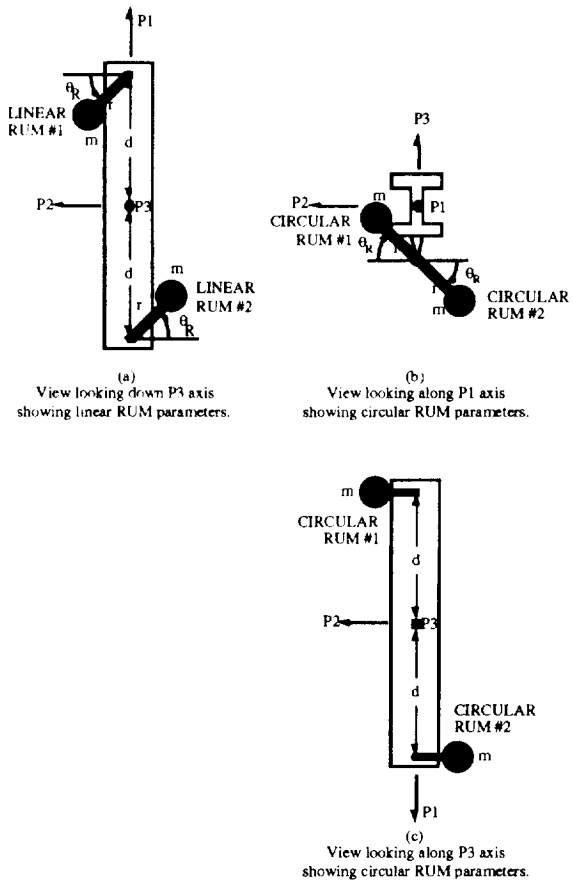

Fig. 3 Definition of the RUM Parameters

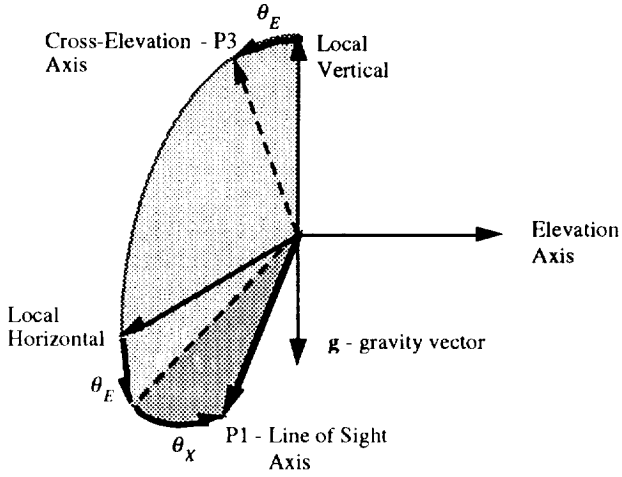

Fig. 4 Definition of the Elevation and Cross-Elevation Gimbal Angles

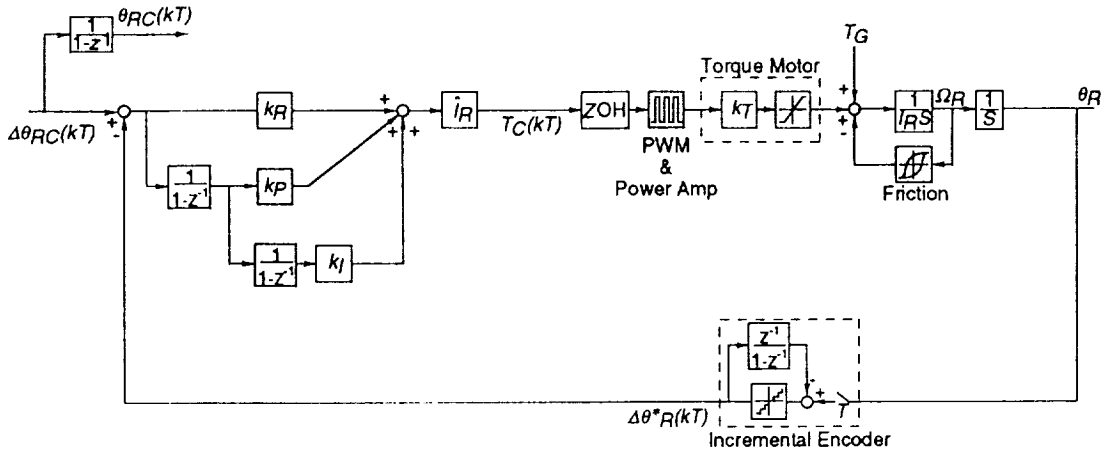

Fig. 5 Control System Block Diagram for the RUM Servos

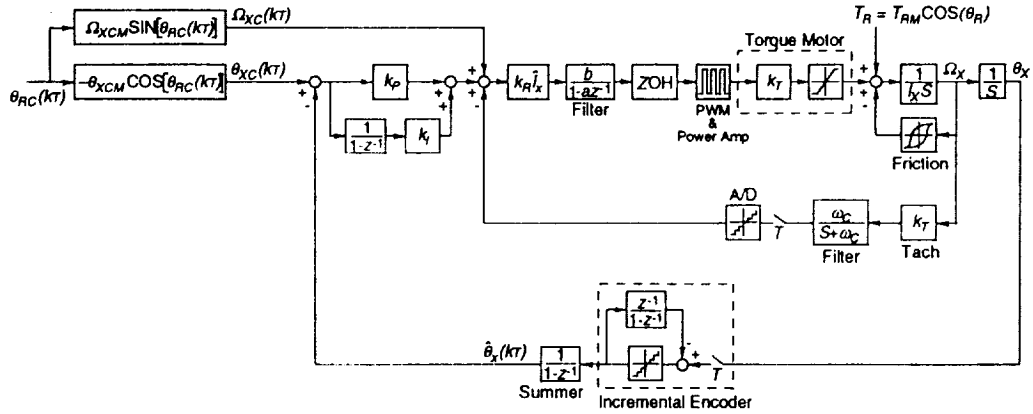

Fig. 6 Control System Block Diagram for the Cross-Elevation Servo

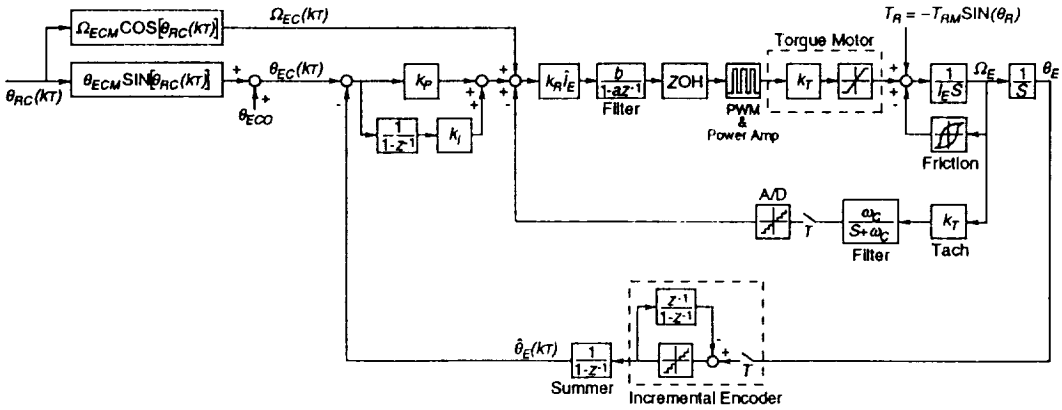

Fig. 7 Control System Block Diagram for the Elevation Servo

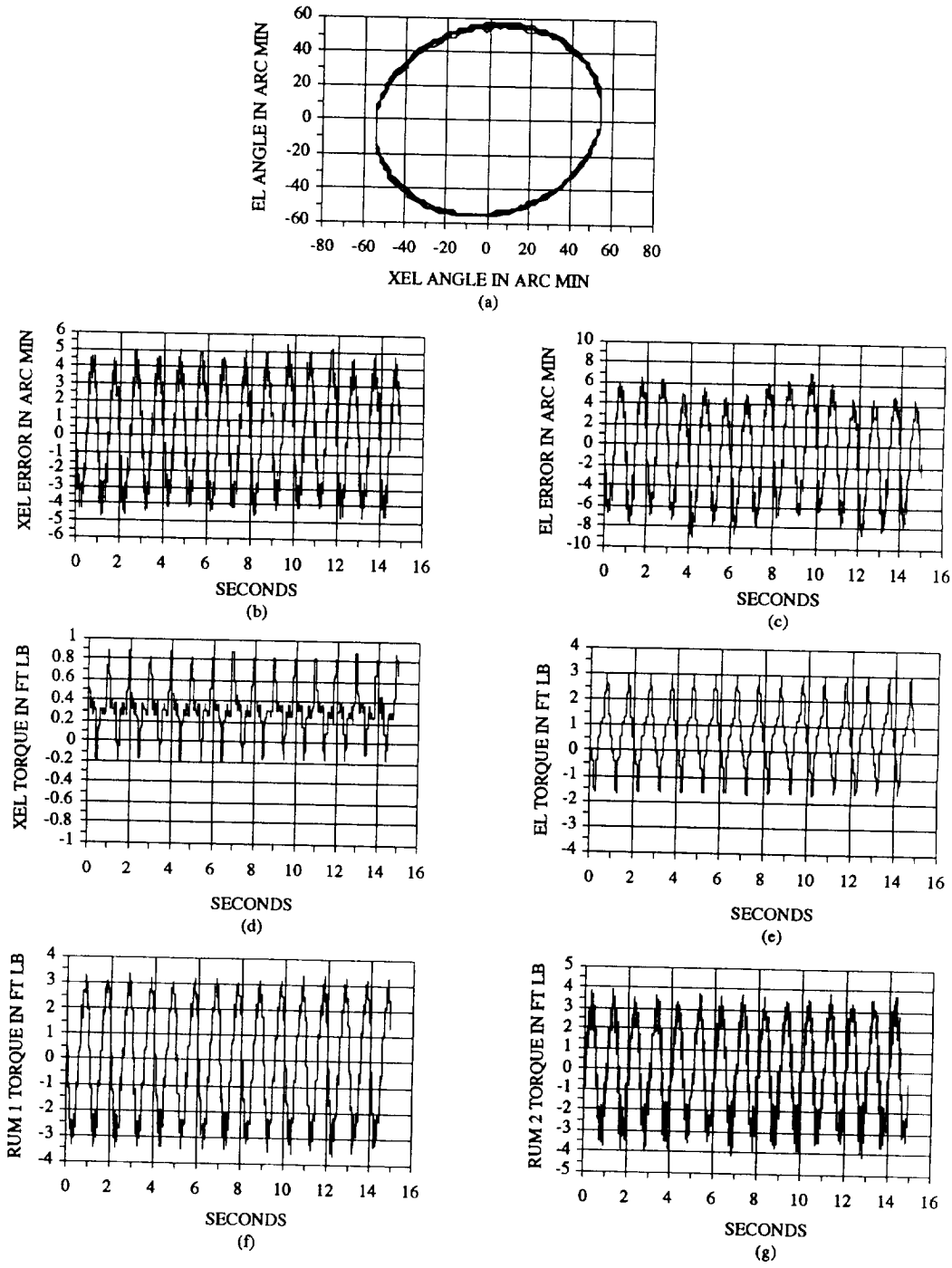

Fig. 8 RUM Experiment Test Results for Circular Scanning With RUM's and Gimbal Servos at 0 deg Elevation Angle

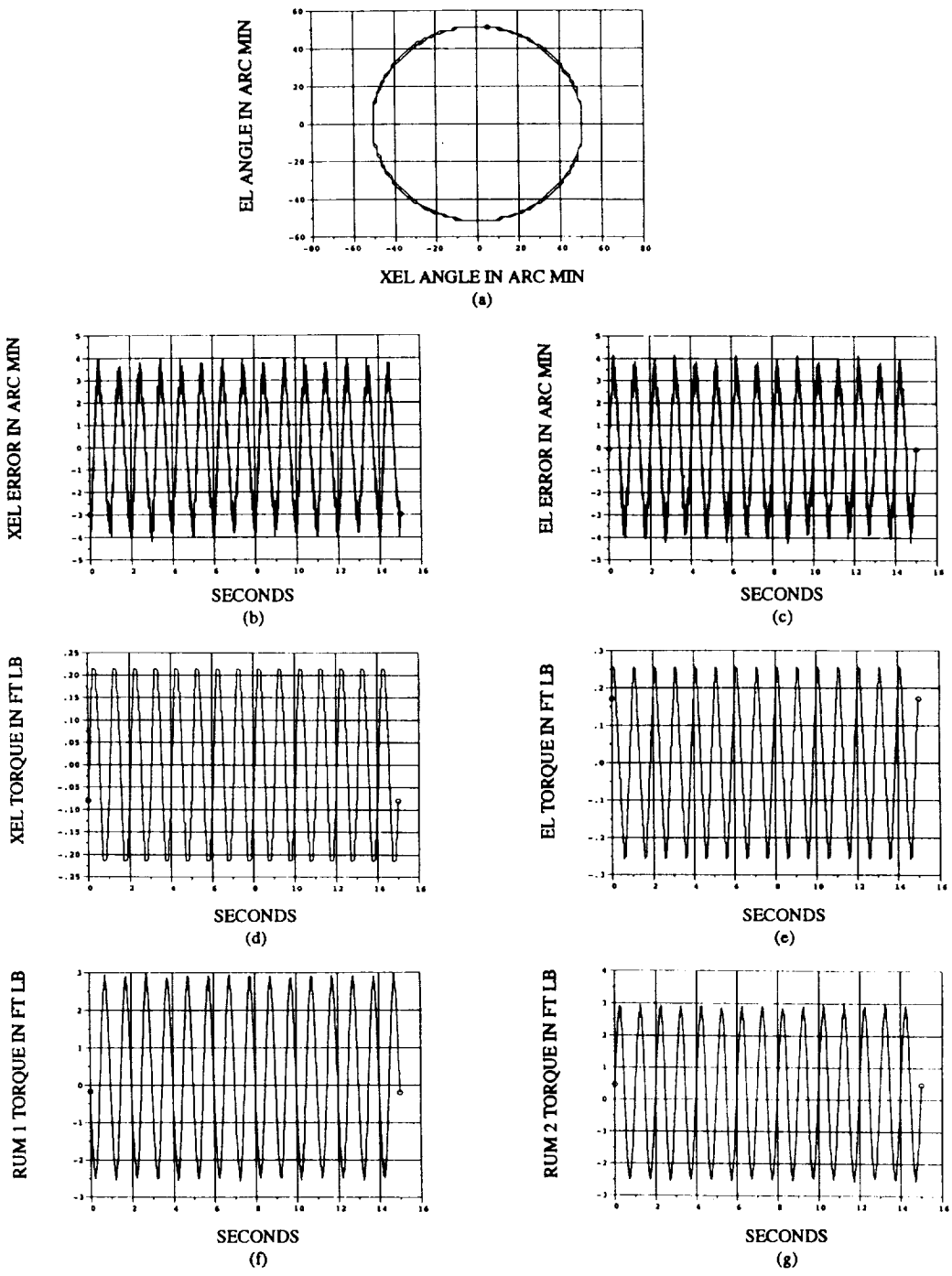

Fig. 9 Computer Simulation Results for Circular Scanning With RUM's and Gimbal Servos at 0 deg Elevation Angle

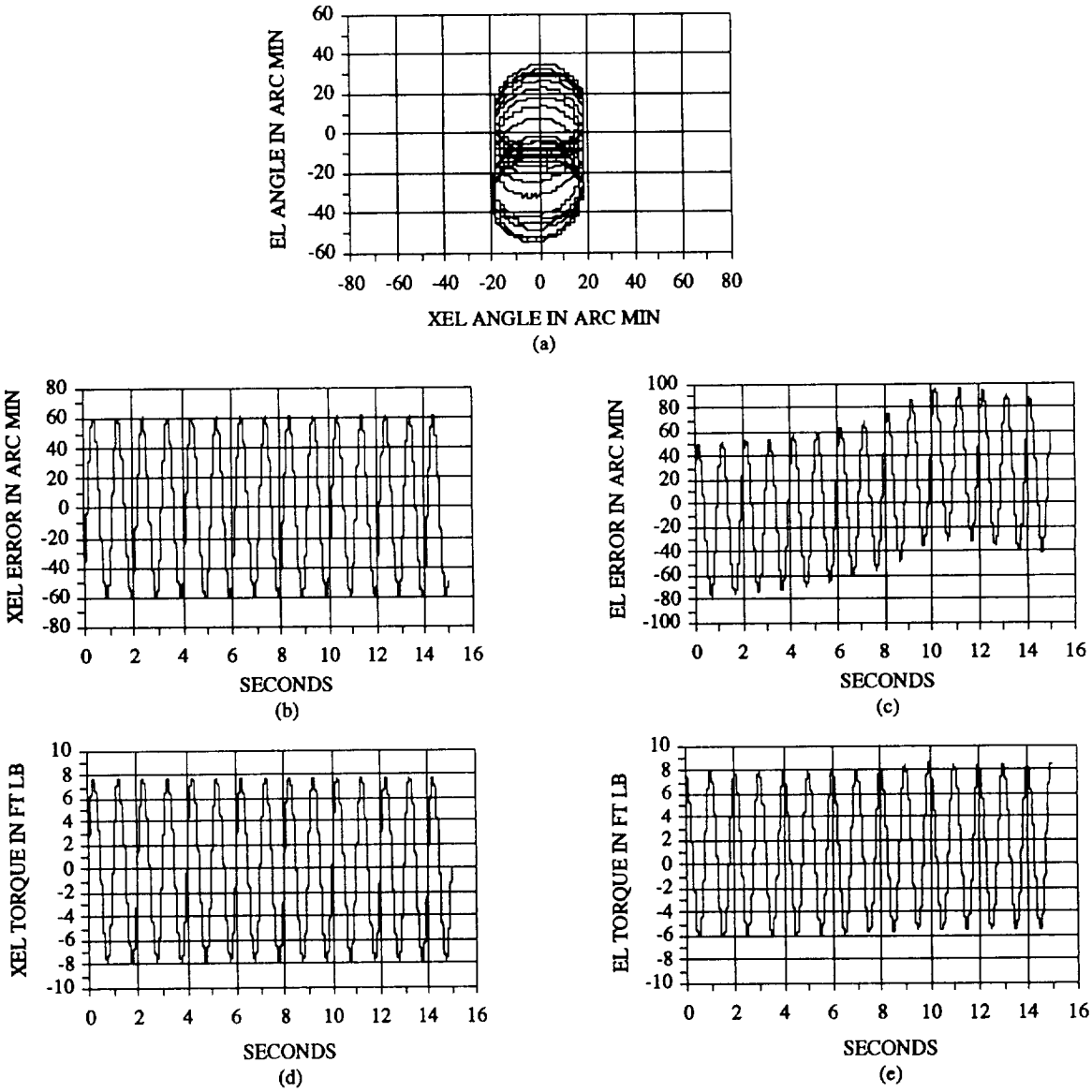

Fig. 10 RUM Experiment Test Results for Circular Scanning With Gimbal Servos Only at 0 deg Elevation Angle

Table 1

SUMMARY OF RESULTS FROM RUM EXPERIMENT FOR LINEAR SCANNING

EL ANGLE, IN DEG	CMD/ACTUAL SCAN AMPLITUDE, IN ARC-MIN	XEL/EL SCAN ERRORS, IN ARC-MIN RMS[2]	TOTAL POWER FOR TRQ MOTORS USED, IN WATTS RMS[3]
RESULTS USING RUM's AND GIMBAL SERVOS:			
0	51/51 (51/51)	1/2 (2/<1)	1 (<1)
-90	51/51 (51/51)	1/1 (2/<1)	29 (21)
RESULTS USING GIMBAL SERVOS ONLY:			
0	51/17 (51/22)	42/2 (42/<1)	79 (49)
0	128/51[4] (128/51)	105/2[4] (105/<1)	494[4] (333)
-90	51/18 (51/22)	42/1 (42/<1)	79 (49)
-90	128/51[4] (128/51)	105/1[4] (105/<1)	494[4] (333)

Table 2

SUMMARY OF RESULTS FROM RUM EXPERIMENT FOR CIRCULAR SCANNING

EL ANGLE, IN DEG	CMD/ACTUAL SCAN RADIUS, IN ARC-MIN	XEL/EL SCAN ERRORS, IN ARC-MIN RMS[2]	TOTAL POWER FOR TRQ MOTORS USED, IN WATTS RMS[3]
RESULTS USING RUM's AND GIMBAL SERVOS:			
0	51/55 (51/51)	3/4 (2/2)	32 (21)
-90	51/55 (51/51)	4/4 (2/2)	4 (<1)
RESULTS USING GIMBAL SERVOS ONLY:			
0	51/18 (51/22)	42/48 (42/42)	147 (99)
0	128/51[4] (128/51)	105/120[4] (105/105)	919[4] (666)
-90	51/20 (51/22)	42/44 (42/42)	144 (99)
-90	128/51[4] (128/51)	105/110[4] (105/105)	900[4] (666)

NOTES:
(1) Top numbers w/o parentheses are actual hardware results; lower numbers in parentheses are computer sim results.
(2) Scan errors are error signals in gimbal servos.
(3) Assumes that bias torques of gimbal torque motors can be cancelled by better mass balancing.
(4) Extrapolated from result above, based on simulation findings. This is necessary because scan cannot be generated with 11 ft-lb gimbal torque motors that are in RUM experiment.